



Published in final edited form as:

*Biofabrication*. ; 7(3): 035001. doi:10.1088/1758-5090/7/3/035001.

## Fabrication of Compositionally and Topographically Complex Robust Tissue Forms by 3D-Electrochemical Compaction of Collagen

Mousa Younesi<sup>1</sup>, Anowarul Islam<sup>1</sup>, Vipuil Kishore<sup>1,2</sup>, Stefi Panit<sup>1</sup>, and Ozan Akkus<sup>1,3,4,\*</sup>

<sup>1</sup>Department of Mechanical and Aerospace Engineering, Case Western Reserve University, Cleveland, OH 44106, United States

<sup>2</sup>Department of Chemical Engineering, Florida Institute of Technology, Melbourne, FL 32901, United States

<sup>3</sup>Department of Biomedical Engineering, Case Western Reserve University, Cleveland, OH 44106, United States

<sup>4</sup>Department of Orthopedics, Case Western Reserve University, Cleveland, OH 44106, United States

### Abstract

Collagen solutions are phase-transformed to mechanically robust shell structures with curvilinear topographies using electrochemically induced pH gradients. The process enables rapid layer-by-layer deposition of collagen-rich mixtures over the entire field simultaneously to obtain compositionally diverse multilayered structures. In-plane tensile strength and modulus of the electrocompacted collagen sheet samples were 5200 -fold and 2300 -fold greater than that of uncompacted collagen samples. Out of plane compression tests showed 27 -fold and fold increase in compressive stress and 46 -fold increase in compressive modulus compared to uncompacted collagen sheets. Cells proliferated 4.9 times faster, and cellular area spread was 2.7 times greater on compacted collagen sheets. Electrocompaction also resulted in 2.9 times greater focal adhesion area than on regular collagen hydrogel. The reported improvements in the cell-matrix interactions with electrocompaction would serve to expedite the population of electrocompacted collagen scaffolds by cells. The capacity of the method to fabricate nonlinear curved topographies with compositional heterogeneous layers is demonstrated by sequential deposition of collagenhydroxyapatite layer over a collagen layer. The complex curved topography of the nasal structure is replicated by the electrochemical compaction method. The presented electrochemical compaction process is an enabling modality which holds significant promise for reconstruction of a wide spectrum of topographically complex systems such as joint surfaces, craniofacial defects, ears, nose or urogenital forms.

\*Corresponding author: Departments of Mechanical and Aerospace Engineering, Biomedical Engineering and Orthopaedics, Case Western Reserve University, 10900 Euclid Avenue, Glennan 615, Cleveland, OH 44106, Tel.: 1-(216)-368-4175, Fax: 1-(216)-368-6445, ; Email: ozan.akkus@case.edu

## Keywords

3D collagen scaffold; biofabrication; electrochemical compaction; cell adhesion; tissue engineering

---

## 1. Introduction

Collagen molecule is the ubiquitous brick that endows many tissues with form and structural soundness. Furthermore, collagen molecules constitute a niche that is conducive to cell adhesion, motility, proliferation and biodegradation. That is why collagen is situated at the center of biomaterial and tissue engineering applications. While the natural collagen-rich tissues have impressive capacity to bear mechanical loads, the mechanical properties of reconstituted collagen have the consistency of a gel; thus, it is generally limited to non-load bearing applications. A major discord between collagen in the native tissue matrix and reconstituted collagen gels is the degree of compaction of the collagen molecules. The former can be as dense as 250–400 mg of collagen per mL [1, 2] of tissue volume whereas gels are in the range of 1–10 mg/mL. While other factors such as non-collagenous proteins and proteoglycans contribute to superior strength of the native collagenous tissue, modalities to increase the packing density of collagen would be an important step in improving this important biomaterial's robustness.

In recognition of the need for more robust collagen products, researchers have devised methods to condense collagen such as plastic compression [3] or prolonged drying [4]. In recent years, it has been demonstrated that solubilized collagen molecules can be compacted isoelectrically by using pH gradients induced by electrolysis of water molecules (Figure 1a) [5,6]. Collagen is an ampholytic molecule which has  $-0.8$  coulombs of charge at  $\text{pH} = 3$  (anode region) and of  $+0.8$  coulombs at  $\text{pH} = 11$  (cathode region). The differential charge results in the repulsion of molecules away from both electrodes. Such repulsion results in the electrochemical compaction of molecules. The molecules have a net charge of zero at the isoelectric point of  $\text{pI} = 8.2$ ; thereby, molecules are condensed at the isoelectric point [5]. Absence of net charge at the  $\text{pI}$  enables the close packing of molecules (Figure 1a & b). The studies thus far have been executed in 1-D by employing wire electrodes to fabricate collagen threads [5–8]. In principle, the same process can generate collagen in the sheet form by using planar electrodes in 2D. More importantly, complex 3D nonlinear surface topographies can be obtained if the electrodes are machined accordingly.

Biofabrication methods that can perform rapid deposition of collagen-rich solutions into dense and curved topographies while elevating the mechanical properties for shape retention at the baseline would be highly significant for dental, craniofacial, urogenital and orthopaedic applications. The current study introduces the electrochemical compaction method for fabrication of collagen based scaffolds with different dimensions and topographies. Effects of electrocompaction process on the mechanical properties of collagen products and response of resident cells with respect to the standard uncompacted collagen gel are investigated. The capacity of electrocompaction as a materials processing modality is demonstrated by fabrication of multilayered hemispherical construct to emulate a striated

structure of the curved joint surface; and fabrication of a geometrically complex nasal shaped scaffold.

## 2. Materials and methods

Purified monomeric atelo-collagen was obtained from Advanced BioMatrix (acid solubilized, type I, 6 mg/mL, San Diego, CA). Type-II collagen (Elastin Products Company, MO) was obtained in powdered form and dissolved in 0.1 N acetic acid solution at a concentration of 3 mg/ml. Molecular collagen solutions were dialyzed against ultrapure water. Chondroitin sulfate (CS; Sigma, MO) was dissolved in ultrapure water at 10 mg/mL concentration and mixed with dialyzed type II collagen at a ratio that mimic the composition of the native cartilage (1:4 CS:type-II collagen, by weight). A mixture of hydroxyapatite microparticles (HA, Sigma-Aldrich) and collagen solution was prepared at 60% w/w ratio.

### Synthesis of Electrochemically Compacted Collagen Products

The electrocompaction method involves loading dialyzed monomeric collagen solution (type I, type II or their mixtures with CS or HA) between linear, planar or curvilinear electrodes and applying an electrical current ( $5 \text{ A/cm}^2$ ) to form densely packed collagen products (Figure 2b–d). Electrodes were separated by silicon rubber spacers (thickness of 2 mm) within which the collagen solution was loaded. Besides containment of the collagen solution, the rubber spacer prevented short circuit. The compaction results in the molecular solution to phase transform as a disc-shaped sheet at a position near the cathode under the effect of physicochemical mechanisms explained previously [8] and as summarized in Figure 1a. The electrocompaction process was executed at the room temperature.

The uncompacted collagen gel was prepared by using the same collagen stock. The gelation was induced by mixing the collagen solution and 10x PBS at a volume ratio of 8 to 1, respectively, and then adjusting the pH to 7.4 by adding 0.1 N NaOH. The solution was loaded into a cylindrical mold and allowed to gel at 37 °C for 2 hours.

**Crosslinking with genipin solution**—Gels and sheets made from type I or type II collagen were crosslinked with 0.625 wt. % genipin in 90 vol. % ethanol solution for 72 hours at 37 °C. Following crosslinking, samples were rinsed with ultrapure water and cut as discs using 5 mm diameter skin biopsy punch to be used in compression tests or as rectangular strips for tensile tests.

**Shrinkage measurement**—Disc-shaped samples of compacted collagen sheets and collagen gel were cut using a biopsy punch with diameter of 10 mm. Samples were incubated at 37 °C for 2 hrs to dry. Diameters of dried samples were measured to calculate the radial shrinkage of samples. Three samples per group were used in measurement and average and standard deviations were reported.

**Degree of Compaction**—The thicknesses of samples were used to assess the degree of compaction. Five mm diameter biopsy punches were used to cut samples from each electrocompacted sheet. Thickness of cross-linked samples was measured after cutting them in to final size using a custom-setup which measures the thickness of the samples based on

electrical conductivity without compressing them. Since the areas of disc-samples were the same (as defined by the biopsy punch), the ratios of thicknesses reflect the degree of volumetric compaction.

**Compressive Mechanical Properties**—The crosslinked uncompacted and compacted collagen discs (type I, type II, type II added with chondroitin sulfate and type I added with HA) were subjected to constant strain-rate out-of-plane compression (Figure 3b) (1%/s) using a Rheometrics Solid Analyzer (RSAII, Rheometrics Inc., Piscataway, NJ, USA) to measure compressive stress and modulus. The maximum stress at 30% strain was reported as the compressive failure stress. Apparent Young's modulus was determined by calculating the slope of stress-strain curve in the vicinity of 10% to 20% strain range by linear regression. All samples were soaked in PBS for 1 hr before the tests. 10 samples from each group were tested and averages and standard deviations are reported. Rabbit and chicken cartilage samples were cut from the tibial plateaus of animals using a 5 mm biopsy punch. Cartilage samples were also soaked in PBS about 1 hr before compression tests and tested as described for collagen samples.

**Tensile Mechanical Properties**—In-plane tensile tests (Figure 3b) were performed on the strips cut out from electrocompacted type-I collagen sheets using a Rheometrics Solid Analyzer (RSAII, Rheometrics Inc., Piscataway, NJ, USA) at a gauge length of 10 mm and a strain rate of 1%/sec. Ultimate tensile strength and apparent Young's modulus were calculated as described for compression test.

**Cell morphology and proliferation**—Compacted and uncompacted type-I collagen sheets were sterilized with 70% ethanol solution overnight, washed with 1x PBS and placed in ultralow attachment 24-well culture plate (Corning). To investigate the effect of electrochemical compaction on cell morphology and proliferation, passage-5 human mesenchymal stem cells (MSCs, Lonza) were seeded at a density of 5000 cells/cm<sup>2</sup> and cultured for 7 days in a culture media composed of  $\alpha$ -MEM with 10% FBS and 1% penicillin/streptomycin. At Day 1 and Day 7, cells were fixed with 3% formalin solution (0.1% triton-x100) and the F-actin filaments were stained with Alexafluor Phalloidin. A multiphoton confocal microscope (Leica TCS SP2) was used to take images of the samples for assessing the cell morphology. Cell counts on compacted and uncompacted collagen sheets were performed on DAPI stained images using ImageJ (U. S. National Institute of Health, Bethesda, MD) to quantify cell proliferation on compacted and uncompacted collagen sheets. Data were analyzed using Student t-test. Statistical significance was set at  $p < 0.05$ .

**Focal adhesion imaging**—Cardiomyocytes (Passage 19) (200,000 in 1 mL of medium) were transduced to produce talin-GFP fusion proteins by mixing with 60  $\mu$ L of *CellLight® Reagents BacMam 2.0* (Life Technologies) and shaken gently for 2 hr at 37 °C. We have used cardiomyocytes instead of MSCs because the latter were not susceptible to transduction. Transduced cardiomyocytes were cultured in glass bottom petri-dish (9.5 cm<sup>2</sup>) overnight. Transduction efficiency was checked by observing the cells under the fluorescent microscope with excitation/emission wavelength of 488/510. After optimizing the efficiency

of transduction process, cells were trypsinized and cultured on collagen gel or electrocompacted sheets overnight. Focal adhesions were observed by a fluorescent microscope (Olympus EX83). ImageJ software was used to measure the spreading areas of the cells on electrocompacted and gel samples from bright field microscopy images. After background correction on fluorescent microscopy images, the areas and fluorescent intensity of focal adhesions were quantified for individual cells (6 cells/group) on electrocompacted and gel samples.

**Layer by layer deposition of curvilinear geometries**—A 12.5 mm diameter hemispherical indent was milled in a carbon electrode as the cathode for making a hemispherical bilayered osteochondral scaffold (Figure 6f–i). The indent was filled with pure collagen solution. An aluminum sphere of 10 mm diameter served as the anode and it was positioned concentrically within the hemispherical indent. Electric current ( $5 \text{ A/cm}^2$ ) was applied to compact the collagen layer on the hemisphere. A mixture of hydroxyapatite microparticles (Sigma-Aldrich) and collagen solution with 60% w/w hydroxyapatite was applied on the top of the electrocompacted collagen layer and electric current was applied to electrocompact the second layer that is emulating the underlying subchondral bone.

For making the nasal template, cathode and anode were made by casting the molten bismuth alloy to the nose region of a plastic face mask (Figures 6j and 6k). The concave anode was filled with collagen and the cathode was fixed on the top of the anode with a separation of 2 mm and electrical current was applied to compact the collagen molecules in the shape of the nose on cathode surface. The process was repeated three times to make a robust scaffold which retained the shape of nose.

**Secondary Electron Microscopy (SEM)**—A compacted collagen sheet made of telocollagen (non D-banded) was fractured under tensile load to expose the thickness of the sample for SEM imaging. D-banded collagen extracted from lamb tendon was used to demonstrate that electrochemical processing does not harm the collagen microstructure. Samples were dried on a glass slide surface dropwise at  $37^\circ \text{C}$ . Samples were fixed on the SEM stub and coated with palladium in a sputter coating device (Denton Desk IV Coater DCH 240). Thickness of the coating was 5 nm. Samples were analyzed with a SEM microscope (FEI Helios 650) with a voltage of 1 kV and beam current of 0.2 nA to investigate the effect of electrocompaction process on microstructure of collagen.

**Assessment of denaturation by circular dichroism**—3 mg of gelatin dissolved in 1 mL of 0.1 N HCl solution. 1 mL of dialyzed collagen with concentration of 6 mg/mL was diluted with 1 mL of 0.2 N HCl to get final concentration of 3 mg/mL for solution. 1 mL of dialyzed collagen solution with concentration of 6 mg/mL was electrocompacted to a sheet and then dissolved in 2 mL of 0.1 N HCl solution to have the final concentration of 3 mg/mL. Different dilutions of all three samples were prepared to find out the appropriate concentration for analysis. Samples with concentration of  $60 \mu\text{g/mL}$  provided acceptable results. A circular dichroism spectrometer (AVIV circular dichroism spectrometer with a 450-watt Suprasil Xenon arc lamp controlled by a high stability, constant current, DC power supply) was used for analysis. The cuvette volume for holding the sample was  $400 \mu\text{L}$ . For each sample the analysis repeated 5 times and the average is reported.

**Statistical Analysis**—The results for cell proliferation ( $n = 5/\text{group}$ ), focal adhesion imaging ( $n=6/\text{group}$ ) and mechanical test ( $n = 10/\text{group}$ ) were analyzed using student's t-test to assess the effects of electrocompaction on properties of collagen products. Statistical significance was set at  $p < 0.05$ .

### 3. Results

As it is visualized schematically (Figure 2 b–d), method is capable of producing product in 1, 2, and 3 dimensions. The thickness of the sheets can be controlled in the range of tens of microns up to few millimeters. The utilization of dilute collagen solutions generates thinner sheets whereas recursive electrocompaction (i.e. fill-compact-fill-compact sequences) results in thicker sheets (Figure 2d). The duration of electrocompaction for each layer is about 60 seconds. Collagen solutions can be mixed with secondary molecules/particles (Figure 2a) which are also convectively encapsulated in the electrocompacted sheet. Furthermore, the composition of each layer can be varied separately during layer-by-layer assembly process. This facet would be critical to constructing gradient interfaces or sequential delivery of therapeutic agents.

Electrocompacted collagen was  $17 \pm 3$  times denser than collagen gels (Figure 3a). The dense structure prevented shrinkage of the compacted collagen sheet in comparison to collagen gel. Compacted collagen sheet showed  $9 \pm 4$  percent radial shrinkage whereas collagen gel shrunk by  $19 \pm 7$  percent. This denser structure affects the mechanical properties of the electrocompacted sheet significantly. The compressive strength and stiffness of electrocompacted sheets were  $27 \pm 7$  -fold and  $46 \pm 7$  -fold higher compared to the uncompacted collagen sheets, respectively (Figure 3c and 3d). Results of tensile test demonstrated greater than three orders of magnitude (5200 -fold) increase in the strength of electrocompacted collagen sheets ( $6.2 \pm 1.6$  MPa) compared to uncompacted collagen sheets ( $<10$  kPa) (Figure 3c–e). The stiffness anisotropy calculated by taking the ratio of the in-plane stiffness (54 MPa) with the out of plane stiffness (0.1 MPa) indicated a 540 -fold difference demonstrating that the electrocompacted collagen sheets are highly anisotropic.

Cell morphology, proliferation and adhesion changed dramatically on electrochemically compacted sheets. The cells seeded on the uncompacted collagen sheets were round and poorly adherent at Day 1 with low levels of focal adhesions (Figure 4a and Figure 5a). On the other hand, the cells on the compact sheet were readily spread (Figure 5b) (2.7 -fold greater cell spreading area) to assume elongated morphology at Day 1 (Figure 4c). Cells on electrocompacted sheets had greater number and bigger focal adhesions (2.9 -fold) and the strength of focal adhesions established by cells were higher (2 -fold) (Figure 5c). Only by Day 7, the elongated morphology appeared on uncompacted sheets (Figure 4b). At Day 7, cells were sparsely distributed on uncompacted sheets (Figure 4b) whereas a confluent cell layer was observed on the electrocompacted sheet (Figure 4d). Cell counts confirmed these observations, showing that cell proliferation was significantly higher (4.9 -fold) on compacted sheets compared to uncompacted sheets (Figure 4e).

The electrocompaction method is not limited to type-I collagen alone. It can also be used to compact other ampholytic molecules that have a rod-like structure (type-II collagen, elastin,

etc.). Highly dense and mechanically robust pure type-II collagen sheets can be synthesized by the electrocompaction method (Figure 2c and Figure 6e). Furthermore, the ELCOM method allows for the incorporation of additional proteoglycans or glycosaminoglycans (such as chondroitin sulfate as demonstrated in Figure 6e) within the collagen sheet by simply mixing the component with the collagen solution at the desired concentration prior to electrochemical compaction [9]. Here, we show that the ELCOM method can be employed to form cartilage analog sheets that mimic the composition of the native cartilage (type-II collagen + 20% chondroitin sulfate) using planar graphite electrodes (Figure 6d). Dimethylmethylene blue (DMMB) staining confirmed the presence of chondroitin sulfate within the type-II collagen sheet (Figure 6e).

A unique aspect of the ELCOM method is the capacity to fabricate geometrically complex structures by using contoured electrodes (Figure 2d). As a proof of concept, a mechanically robust bilayered scaffold with curved topography was fabricated by employing carbon block electrodes containing a hemispherical indent as the cathode and an aluminum ball as the anode (Figure 6f and 6g). The bilayered scaffold was comprised of a collagen layer and the mineral layer. The collagen layer of the scaffold was formed by filling the hemispherical indent with the collagen solution, positioning the aluminum ball concentrically over the hemispherical indent and applying the electric current. The resulting electrocompacted structure was in the form of a hemispherical shell deposited on the cathode. For the mineral layer, the indent was successively filled with a mixture of collagen solution suspended with hydroxyapatite particles (60 wt% HA) and electric current was applied again. The resulting product was removed and crosslinked in genipin solution for two hours to obtain the final hemispherical bilayered shell. Results (Figure 6h and 6i) demonstrate the ability of the ELCOM method to generate: a) multiphasic (cartilage-like layer deposited over bone-like layer), b) non-planar geometries. When molten metal was molded as electrodes that match the shape of the nasal structure (Figure 6j and 6k) it was possible to replicate the structure as a shell that maintained its form (Figure 6l and 6m). This nasal construct clearly demonstrates the potential of the method to fabricate anatomically conforming constructs

#### 4. Discussion

Electrochemical compaction (ECOM) method is unique in providing robust collagen constructs in 1D, 2D, and 3 dimensions. The deposition occurs rapidly and simultaneously over the entire electrode surface in a minute-long time frame. Since the cell based approaches for fabricating the collagen construct are generally time consuming, having a fast method of making collagen construct with acceptable baseline mechanics is highly significant. The thickness of the sheets can be controlled in the range of tens of microns up to few millimeters by adjusting the amount of collagen loaded between electrodes. The utilization of recursive electrocompaction (i.e. fill-compact-fill-compact sequences) results in thicker sheets (Figure 2d). Collagen solutions can be mixed with secondary molecules/particles (Figure 2a) which are also convectively encapsulated in the electrocompacted sheet. Furthermore, the composition of each layer can be varied separately during layer-by-layer assembly process. This facet would be critical to constructing gradient interfaces or sequential delivery of therapeutic agents. There are other layer by layer fabrication techniques such as stereolithography [10], selective laser sintering [11], and different 3D

printing techniques [12–14]. These methods work with many materials but not with collagen at the level of mechanical robustness we report with ECOM. For instance, Hashimdeen et al. [12] fabricated an ear-like construct with a custom designed printer using polycaprolactone. ECOM process provides a close control of the 3D topography as shown by the nose-like scaffold because the collagen is deposited on the electrode and resulting scaffold follows the shape of the electrode closely (Figure. 5). An advantage of ECOM is rapidity. The entire scaffold is compacted over the full field within one minute. 3D Printing modalities employ point by point deposition and fabrication may take hours depending on the size and resolution employed.

In ECOM method, composition of compacted sheet can be changed layer by layer to make a sudden or gradual change in construct composition. As we showed, a bone-like composition of collagen with 60% hydroxyapatite mineral particle was fabricated on top of other layer of pure collagen in fabrication of a hemispherical construct (Figure 5c). Also, a compacted sheet of layer with 20% chondroitin sulfate with collagen type II was fabricated to mimic the native cartilage composition (Figure 5b). These two examples clarify the versatility of composition which can be processed via electrochemical compaction process to a robust product.

ECOM process does not harm collagen molecules unlike electrospinning [15]. We confirmed the absence of denaturation by assessing the secondary structure of collagen via circular dichroism [16, 17]. Circular dichroic spectra of (Figure 8a) collagen before and after electrocompaction process did not differ while there was a big difference between the gelatin spectrum and collagen spectra. As it can be seen (Figure 8a), the intensity of negative peak for gelatin spectrum was much smaller than that of collagen spectra before and after electrocompaction. Furthermore, the positive peak in gelatin's CD spectrum was missing while this peak was prominent in collagen spectra before and after electrocompaction. Besides collagen molecules, electrocompaction can be performed on D-banded collagen fibers. Electron microscope images (Figure 8b & c) of D-banded collagen fibers before and after electrocompaction confirm the preservation of the D-banding pattern. Therefore, the electrochemical gradients are not harmful to the native organization of collagen molecules.

The ECOM can fabricate aligned collagen threads with a variety of controlled thickness ranging between 50 to 200  $\mu\text{m}$  [8]. In our previous work, the aligned collagen thread was extensively characterized extensively with different analyzing techniques morphologically, structurally, and mechanically [6, 8, 18]. we showed the tensile strength (55 MPa) and Young's modulus (450 MPa) of aligned collagen thread is comparable with the native tendon strength [8]. Furthermore feasibility of fabrication a woven collagen scaffold for use in tendon and ligament tissue engineering was illustrated [8]. Electrospinning and centrifugal spinning are other leading methods of making fibers products and fiber based mats. Products resulting from these processes can have thickness values ranging from 50 nm to 10  $\mu\text{m}$  and comparatively the threads in this work are substantially thicker. Electrospinning is effective for synthetic polymers; however, electrospun collagen products are partially aligned at best with inferior mechanical strength compared to native tissue [19, 20]. Also, there is a high chance of denaturation and gelatinization of collagen during electrospinning process [15]. In contrast, electrochemical aligning of collagen does not harm the collagen microstructure. As

we mentioned before, the strength of the electrochemically aligned collagen threads are close to that of native tissues. In previous work, we have shown that the threads and resultant woven scaffolds can be used in tissue engineering of tendon and ligaments with highly aligned microstructure [8]. Centrifugal spinning has been applied to synthetic polymers such as polyacrylonitrile (PAN) [21], polycaprolactone (PCL), polymethylmethacrylate (PMMA) [22], polystyrene (PS) [23], polyvinylpyrrolidone (PVP), polylactic acid (PLA) [24], and polyethyleneoxide (PEO) [25]. To the best of our knowledge there are no reports on centrifugal spinning being applied to collagen; however, it is plausible that centrifugal spinning may work for aligning and compacting collagen.”

In a different approach Brown et al. [3] obtained condensed collagen sheets by plastic compression where the water content of the collagen gel is reduced by prolonged compression loading. Extrusion or electrospinning of collagen solutions [26, 27] are other methods of making collagen fibers with different thicknesses ranging from nano to micron size scales. Extrusion process can generate threads only whereas the electrospinning can denature collagen [15]. However, as shown in this study ECOM process preserves native collagen structure and it provides a range of scaffold forms from 1D to 3D.

It has also been demonstrated that mitosis occurs more readily on stiffer substrates [22, 23]. Therefore, the order of magnitude increase in substrate stiffness is the likely one of keys effector of increased proliferation on electrocompacted sheets. Factors other than stiffness may have played a role in the observed improvements in proliferation, adhesion and spread of cells. In addition to stiffness, the electrocompaction process is likely to change the topography and the packing density of collagen molecules. Collagen presents ligands for cellular integrins to bind. Process of cell attachment comprises [28] cell spreading, organization of actin cytoskeleton, and formation of focal adhesions. It was shown that [29–32] increasing ligand density or decreasing ligand spacing on the material surface will promote a greater number and stronger focal adhesions.

It was also shown that cell proliferation has a positive relation with cell attachment and spreading area [33]. Based on these results, it can be concluded that increasing the density of bonding ligand will improve the cell attachment and spreading and consequently will improve the cell proliferation. Our results (Figure 3a) show ECOM process to increase the density of collagen solution 17 times. This increase in physical density is very likely to decrease the collagen fiber spacing. Therefore, ECOM process modifies the surface topography and increase the ligand density, improving the cell attachment and spreading on collagen sheet (Figure 6c). As it can be seen in electron microscope images even with a high degree of compaction collagen fibers are visible in surface of sheets with nano dimension porosity (Figure 7b) as well as the bulk of the compacted sheet (Figure 7c). It is likely that the electrocompaction positions collagen molecules in closer proximity which results in the presentation of cell adhesion sites in a denser form, promoting the cell attachment. It has also been demonstrated that mitosis occurs more readily on stiffer substrates [34, 35]. Therefore, the order of magnitude increase in substrate stiffness is the likely effector of increased proliferation on electrocompacted sheets.

To the best of our knowledge, prior literature has not reported gelation of type-II collagen in pure form, a type of collagen that is specific to cartilage. Most type-II collagen scaffolds have been constituted in the presence of secondary polymeric phase [6, 32] or by freeze drying [36] in porous sponge forms. We demonstrated the ability of the ECOM method in fabrication of robust sheet of collagen type II in pure form.

Sculpting collagen-rich structures in 3D curved topographies which can retain their shape is more challenging than synthetic polymers. Synthetic polymers can endure a broad range of physical, thermal and chemical conditions to be molded, machined or cast in various morphologies. In contrast, collagen is a delicate protein which generally does not tolerate conditions which perturb significantly from the physiological state. Collagen is known to denature above 45 °C [37, 38]. Planar deposition of collagen solution in a rapid prototyping context has been possible only after the inclusion of a secondary polymer phase [14, 39, 40]. However, pure collagen stock has not been formed as curved topographies that can retain their shape to date. Another approach to shape collagen rich mixtures into complex shapes is by molding collagen in the gel form as was shown in tissue engineering of the ear [41]. However, the consistency of the gel does not allow shape retention at the baseline and requires long *in vitro* culturing periods to gain structural robustness. Therefore, the reported electrochemical compaction method for rapid fabrication of geometrically complex features in mechanically robust forms is highly significant. Cell studies proved the merit of electrocompacted collagen products over collagen gel from the proliferation rate and cell adhesion points of view.

Electrochemical compaction method is a rapid and straightforward method for fabrication of collagenous constructs with different dimensions and sizes. The electrocompaction process of collagen solution to a robust compacted collagen construct occurs in less than a minute, creating the potential for scaled up production. For instance, it is technically possible to use large electrodes (e.g. 1 × 1 m) to stamp collagen large sized sheets which can be cut to size or arrays of electrodes patterned for the final desired dimensions can be daisy chained for mass electrostamping of multiple sheets simultaneously. The method calls for electrodes and low voltage supply (~10 V); therefore, the investment for setting up a production line would not be costly. The size of product (e.g. diameter of threads or thickness of sheets) can be controlled by changing the amount of collagen and the degree to which they are compacted by modulating the current density. For the fabrication of threads, we have shown the diameter of the threads to be consistent within 5% in a prior publication [8]. In the future, computed tomography or magnetic resonance scanning can be used for machining electrode pairs to generate patient specific scaffolds. A limitation of electrochemical compaction method is the inability to add the cells at the time of fabrication. This is mainly because the electrochemical effect requires salt-free dialyzed collagen solution which limits cell viability due to osmotic pressure. Therefore, strategies using electrochemical compaction would need to introduce cells after scaffold fabrication. This can be accomplished layer by layer addition of cells in the case of sheets and cells can be seeded on threads. Electrochemical compaction is a cutting-edge technology with significant potential to be used for mass production of morphologically challenging systems in the musculoskeletal, craniofacial, dental and urogenital realms for clinical applications as well as research purposes.

## Supplementary Material

Refer to Web version on PubMed Central for supplementary material.

## Acknowledgments

We thank Dr. Anna Akkus for providing collagen solution used for the fabrication of the nasal scaffold. The study was partially funded by the research grant 1306665 co-funded by the CBET and BMAT programs of the National Science Foundation and National Institutes of Health (Grant Number R01 AR063701). Support from the AO Foundation is also gratefully appreciated.

## References

1. Jozsa, LGKP. Human tendons: anatomy, physiology, and pathology. Human Kinetics; Champaign, IL: 1997.
2. Woo SL, Debski RE, Zeminski J, Abramowitch SD, Saw SS, Fenwick JA. Injury and repair of ligaments and tendons. Annual review of biomedical engineering. 2000; 2:83–118.
3. Robert A, Brown MW, Chuo Cher-Bing, Cheema Umer, Nazhat Showan N. Ultrarapid Engineering of biomimetic Materials and Tissues: Fabrication of Nano- and Microstructures by Plastic Compression. Advanced Functional Materials. 2005; 15:9.
4. Guille MMG, Helary C, Vigier S, Nassif N. Dense fibrillar collagen matrices for tissue repair. Soft Matter. 2010; 6:4963–7.
5. Uquillas JA, Akkus O. Modeling the electromobility of type-I collagen molecules in the electrochemical fabrication of dense and aligned tissue constructs. Annals of biomedical engineering. 2012; 40:1641–53. [PubMed: 22314838]
6. Cheng X, Gurkan UA, Dehen CJ, Tate MP, Hillhouse HW, Simpson GJ, et al. An electrochemical fabrication process for the assembly of anisotropically oriented collagen bundles. Biomaterials. 2008; 29:3278–88. [PubMed: 18472155]
7. Abu-Rub MT, Billiar KL, van Es MH, Knight A, Rodriguez BJ, Zeugolis DI, et al. Nano-textured self-assembled aligned collagen hydrogels promote directional neurite guidance and overcome inhibition by myelin associated glycoprotein. Soft Matter. 2011; 7:2770–81.
8. Mousa Younesi AI, Kishore Vipuil, Anderson James M, Akkus Ozan. Tenogenic Induction of Human MSCs by Anisotropically Aligned Collagen Biotextiles. Advanced Functional Materials. 2014
9. Kishore V, Paderi JE, Akkus A, Smith KM, Balachandran D, Beaudoin S, et al. Incorporation of a decorin biomimetic enhances the mechanical properties of electrochemically aligned collagen threads. Acta biomaterialia. 2011; 7:2428–36. [PubMed: 21356334]
10. Cooke MN, Fisher JP, Dean D, Rimnac C, Mikos AG. Use of stereolithography to manufacture critical-sized 3D biodegradable scaffolds for bone ingrowth. Journal of biomedical materials research Part B, Applied biomaterials. 2003; 64:65–9. [PubMed: 12516080]
11. Tan KH, Chua CK, Leong KF, Cheah CM, Cheang P, Abu Bakar MS, et al. Scaffold development using selective laser sintering of polyetheretherketone-hydroxyapatite biocomposite blends. Biomaterials. 2003; 24:3115–23. [PubMed: 12895584]
12. Hashimdeen SH, Miodownik M, Edirisinghe MJ. The Design and Construction of an Electrohydrodynamic Cartesian Robot for the Preparation of Tissue Engineering Constructs. PloS one. 2014:9.
13. Gupta A, Seifalian AM, Ahmad Z, Edirisinghe MJ, Winslet MC. Novel electrohydrodynamic printing of nanocomposite biopolymer scaffolds. J Bioact Compat Pol. 2007; 22:265–80.
14. Kim YB, Kim G. Rapid-prototyped collagen scaffolds reinforced with PCL/beta-TCP nanofibres to obtain high cell seeding efficiency and enhanced mechanical properties for bone tissue regeneration. J Mater Chem. 2012; 22:16880–9.
15. Zeugolis DI, Khew ST, Yew ES, Ekaputra AK, Tong YW, Yung LY, et al. Electro-spinning of pure collagen nano-fibres - just an expensive way to make gelatin? Biomaterials. 2008; 29:2293–305. [PubMed: 18313748]

16. Circular Dichroism: Principles and Applications. VCH; 1994. illustrated
17. Nam K, Kimura T, Kishida A. Controlling coupling reaction of EDC and NHS for preparation of collagen gels using ethanol/water co-solvents. *Macromolecular bioscience*. 2008; 8:32–7. [PubMed: 18023082]
18. Alfredo Uquillas J, Kishore V, Akkus O. Genipin crosslinking elevates the strength of electrochemically aligned collagen to the level of tendons. *Journal of the mechanical behavior of biomedical materials*. 2012; 15:176–89. [PubMed: 23032437]
19. Shields KJ, Beckman MJ, Bowlin GL, Wayne JS. Mechanical properties and cellular proliferation of electrospun collagen type II. *Tissue Eng*. 2004; 10:1510–7. [PubMed: 15588410]
20. Huang ZM, Zhang YZ, Ramakrishna S, Lim CT. Electrospinning and mechanical characterization of gelatin nanofibers. *Polymer*. 2004; 45:5361–8.
21. Khamforoush MTA. A Modified Electro-Centrifugal Spinning Method to Enhance the Production Rate of Highly Aligned Nanofiber. *Nano*. 2015; 10:1550016.
22. Zhang XW, Lu Y. Centrifugal Spinning: An Alternative Approach to Fabricate Nanofibers at High Speed and Low Cost. *Polym Rev*. 2014; 54:677–701.
23. Wang L, Shi J, Liu L, Secret E, Chen Y. Fabrication of polymer fiber scaffolds by centrifugal spinning for cell culture studies. *Microelectron Eng*. 2011; 88:1718–21.
24. Ren L, Pandit V, Elkin J, Denman T, Cooper JA, Kotha SP. Large-scale and highly efficient synthesis of micro- and nano-fibers with controlled fiber morphology by centrifugal jet spinning for tissue regeneration. *Nanoscale*. 2013; 5:2337–45. [PubMed: 23392606]
25. Mahalingam S, Edirisinghe M. Forming of Polymer Nanofibers by a Pressurised Gyration Process. *Macromol Rapid Comm*. 2013; 34:1134–9.
26. Caves JM, Kumar VA, Wen J, Cui W, Martinez A, Apkarian R, et al. Fibrillogenesis in continuously spun synthetic collagen fiber. *Journal of biomedical materials research Part B, Applied biomaterials*. 2010; 93:24–38.
27. Kato YP, Silver FH. Formation of Continuous Collagen-Fibers - Evaluation of Biocompatibility and Mechanical-Properties. *Biomaterials*. 1990; 11:169–75. [PubMed: 2350553]
28. LeBaron RG, Athanasiou KA. Extracellular matrix cell adhesion peptides: functional applications in orthopedic materials. *Tissue Eng*. 2000; 6:85–103. [PubMed: 10941205]
29. Banerjee P, Irvine DJ, Mayes AM, Griffith LG. Polymer latexes for cell-resistant and cell-interactive surfaces. *Journal of biomedical materials research*. 2000; 50:331–9. [PubMed: 10737874]
30. Kantlehner M, Schaffner P, Finsinger D, Meyer J, Jonczyk A, Diefenbach B, et al. Surface coating with cyclic RGD peptides stimulates osteoblast adhesion and proliferation as well as bone formation. *Chembiochem : a European journal of chemical biology*. 2000; 1:107–14. [PubMed: 11828404]
31. Bosnakovski D, Mizuno M, Kim G, Takagi S, Okumura M, Fujinaga T. Chondrogenic differentiation of bovine bone marrow mesenchymal stem cells (MSCs) in different hydrogels: Influence of collagen type II extracellular matrix on MSC chondrogenesis. *Biotechnol Bioeng*. 2006; 93:1152–63. [PubMed: 16470881]
32. Calderon L, Collin E, Velasco-Bayon D, Murphy M, O'Halloran D, Pandit A. Type II collagen-hyaluronan hydrogel--a step towards a scaffold for intervertebral disc tissue engineering. *European cells & materials*. 2010; 20:134–48. [PubMed: 20821371]
33. Chen CS, Mrksich M, Huang S, Whitesides GM, Ingber DE. Geometric control of cell life and death. *Science*. 1997; 276:1425–8. [PubMed: 9162012]
34. Cavalcanti-Adam EA, Micoulet A, Blummel J, Auernheimer J, Kessler H, Spatz JP. Lateral spacing of integrin ligands influences cell spreading and focal adhesion assembly. *European journal of cell biology*. 2006; 85:219–24. [PubMed: 16546564]
35. Koo LY, Irvine DJ, Mayes AM, Lauffenburger DA, Griffith LG. Co-regulation of cell adhesion by nanoscale RGD organization and mechanical stimulus. *Journal of cell science*. 2002; 115:1423–33. [PubMed: 11896190]
36. Ko CS, Huang JP, Huang CW, Chu IM. Type II collagen-chondroitin sulfate-hyaluronan scaffold cross-linked by genipin for cartilage tissue engineering. *Journal of bioscience and bioengineering*. 2009; 107:177–82. [PubMed: 19217557]

37. Zhang ZK, Li GY, Shi B. Physicochemical properties of collagen, gelatin and collagen hydrolysate derived from bovine limed split wastes. *J Soc Leath Tech Ch.* 2006; 90:23–8.
38. Bischof JC, He X. Thermal stability of proteins. *Annals of the New York Academy of Sciences.* 2005; 1066:12–33. [PubMed: 16533916]
39. Xu W, Wang XH, Yan YN, Zheng W, Xiong Z, Lin F, et al. Rapid prototyping three-dimensional cell/gelatin/fibrinogen constructs for medical regeneration. *J Bioact Compat Pol.* 2007; 22:363–77.
40. Cui TK, Wang XH, Yan YN, Zhang RJ. Rapid Prototyping a Double-layer Polyurethane-collagen Conduit and its Schwann Cell Compatibility. *J Bioact Compat Pol.* 2009; 24:5–17.
41. Reiffel AJ, Kafka C, Hernandez KA, Popa S, Perez JL, Zhou S, et al. High-fidelity tissue engineering of patient-specific auricles for reconstruction of pediatric microtia and other auricular deformities. *PLoS one.* 2013; 8:e56506. [PubMed: 23437148]

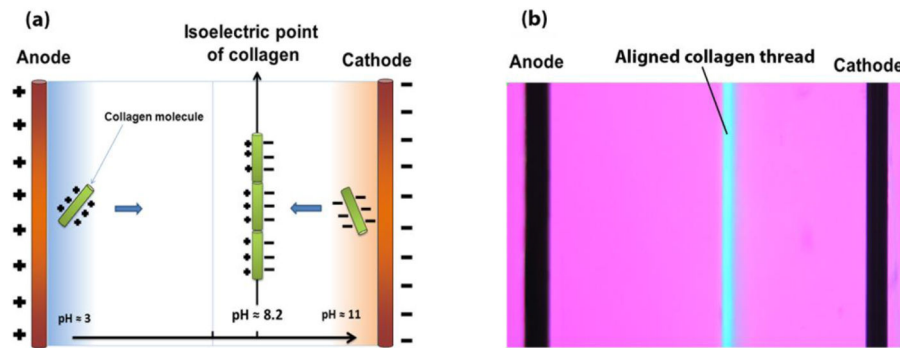


**Figure 1. Principle of electrocompaction process**

(a) schematic of electrochemical alignment of collagen molecules. Collagen molecules between the cathode and anode assume different charges, depending on the local pH. They become negatively charged in basic pH near cathode and positively charged near anode in acidic pH. Since collagen molecules have similar charges with electrodes, a repulsive force condenses molecules at isoelectric point where the net charge of collagen molecules is zero.

(b) Polarized microscopy visualizes the alignment of collagen molecules in isoelectric point of electrochemical cell. Uniform molecular orientation is manifested in blue at the isoelectric point.

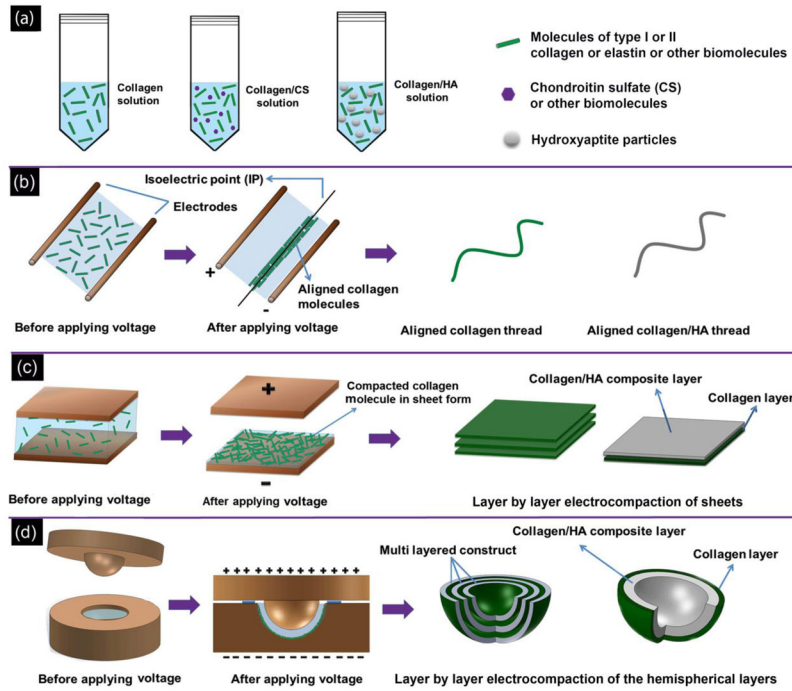


**Figure 2. Overview of the electrochemical compaction process in 1D, 2D and 3D**

Schema of collagen compaction in an electrochemical cell (a), the stock solutions for the process can be pure collagen (type-I or II monomeric solutions), or combinations of collagen solution with mineral particles, glycosaminoglycans or growth factors (b), Execution of the electrocompaction process in 1D to obtain threads (c), 2D to generate planar sheets (d), and in 3D to sculpt curvilinear geometries (e).

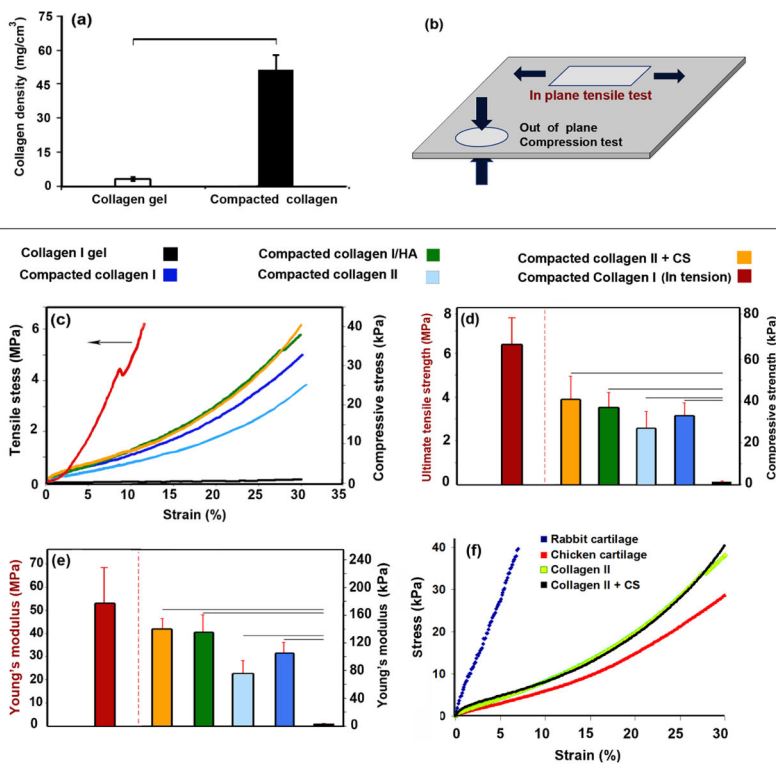


**Figure 3. Electrocompaction increased the mechanical properties of crosslinked collagen sheets by an order of magnitude in compression and three order of magnitude in tension** Collagen density increased substantially as a result of electrocompaction (a), a schematic representation of the material axes along which the tensile and compression tests were performed (b), typical stress strain curves (c), failure strength (d) and Young's moduli values for uncompact collagen gel and electrochemically compacted sheets of various compositions (e). Red curve and bars in b, c, and d show the tensile properties on the left-hand y-axis and compressive properties on the right-hand y-axis (f) Stress-strain curve resulting from compression test of compacted collagen II sheet is on par with the native cartilage. Significant differences between groups in bar graphs are highlighted by black lines.

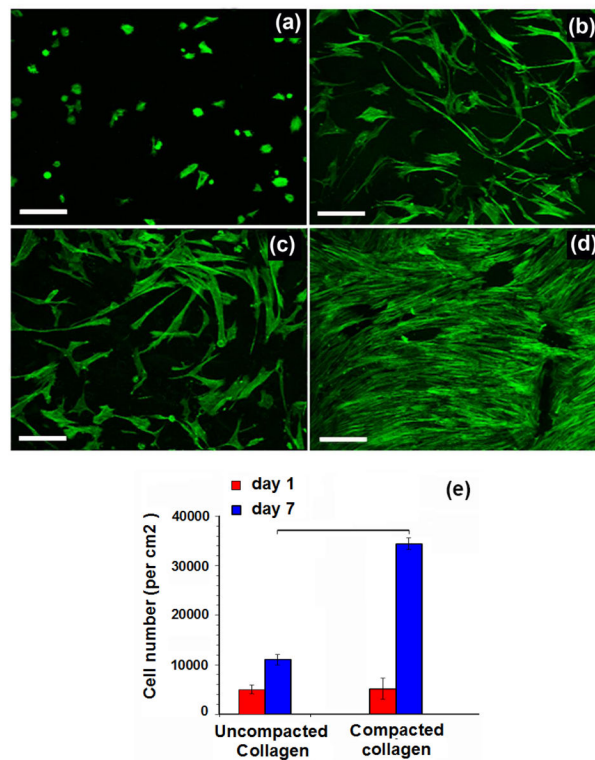


**Figure 4. Electrocompaction of collagen improved cell proliferation and adhesion**

On day 1, (a) cells on collagen gel sheets were round and they were delayed in forming focal adhesions. Only by day 7, (b) cells on collagen gels were able to spread to form a sparsely populated distribution whereas cells on electrocompacted sheets readily established focal adhesions at the same time point (c). On day 7, cells on electrochemical compacted sheets neared confluence (d). Cell numbers on days 1 and 7 on collagen gel and compacted collagen samples (e). (All scale bars: 200  $\mu$ m).

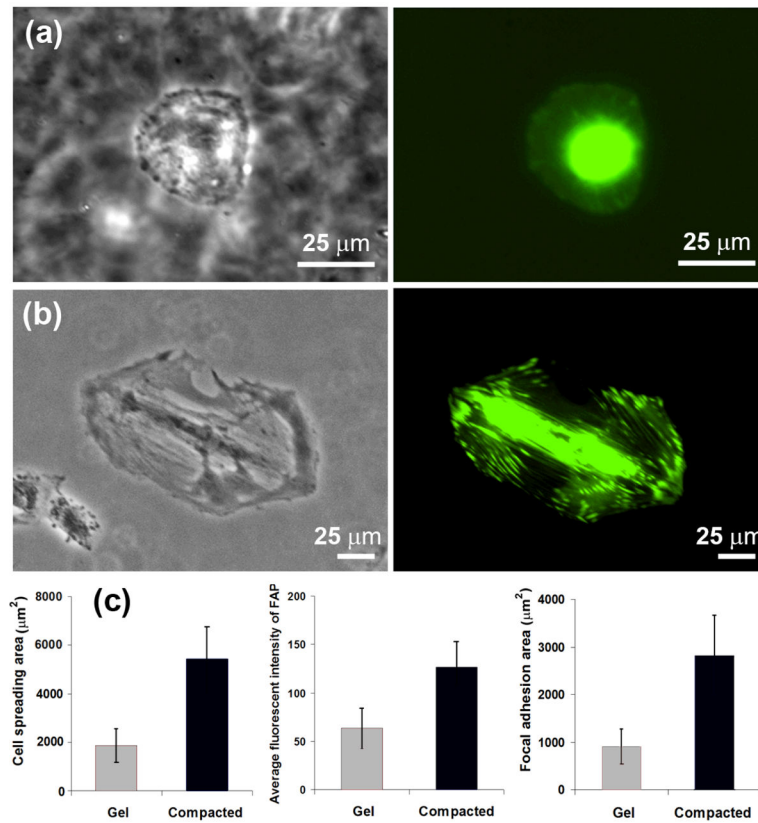


**Figure 5. Focal adhesions of cells on compacted collagen sheet are more strongly present than uncompact collagen gel**

Focal adhesions are visualized by talin-green fluorescent protein fusion *in situ*. Focal adhesions of cells on random collagen gel (a) and compacted collagen sample (b). Cells are more polarized on electrocompacted sheet (a vs. b). Focal adhesions are more mature, stronger, and present in greater amounts on electrocompacted sheets than they are on collagen gel as reflected by greater amount of fluorescent intensity values (c). (All scale bars:  $25\mu\text{m}$ ).

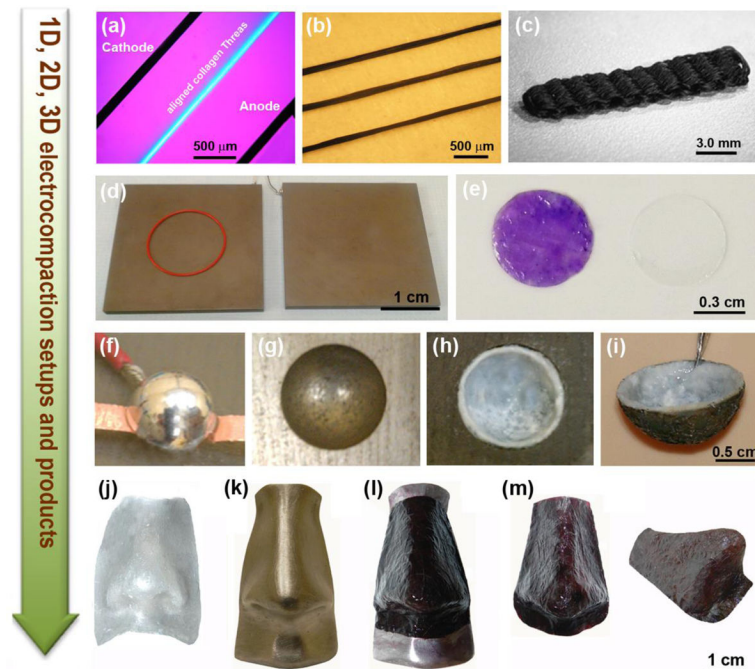


**Figure 6. Biofabrication of a range of electrochemically compacted products**

One dimensional electrocompaction of collagen results in aligned collagen thread (a). Three of these aligned collagen threads (b) can be twisted and woven to obtain 3-dimensional scaffolds for repair of load bearing tissues such as ligaments/tendons (c). Planar graphite electrodes for the production of collagen sheets (d), type-II collagen sheet fabricated by electrochemical processing (e) (left, collagen sheet incorporated with chondroitin sulfate (CS) where CS presence is confirmed by DMMB. Right: pure collagen sheet is transparent as evident by the print design beneath the sheet). (f–i) Construction of a bilayered hemispherical structure that is formed by sequential deposition of a pure collagen layer followed by a collagen-hydroxyapatite layer, emulating a curvilinear osteochondral scaffold. (j–m) A freely standing electrocompacted nasal form electrocompacted by using molded molten metal electrodes (g-female and h-male electrode). The deposition was performed on the male electrode where the nasal collagen-sheet was stained to render it visible (l and m).

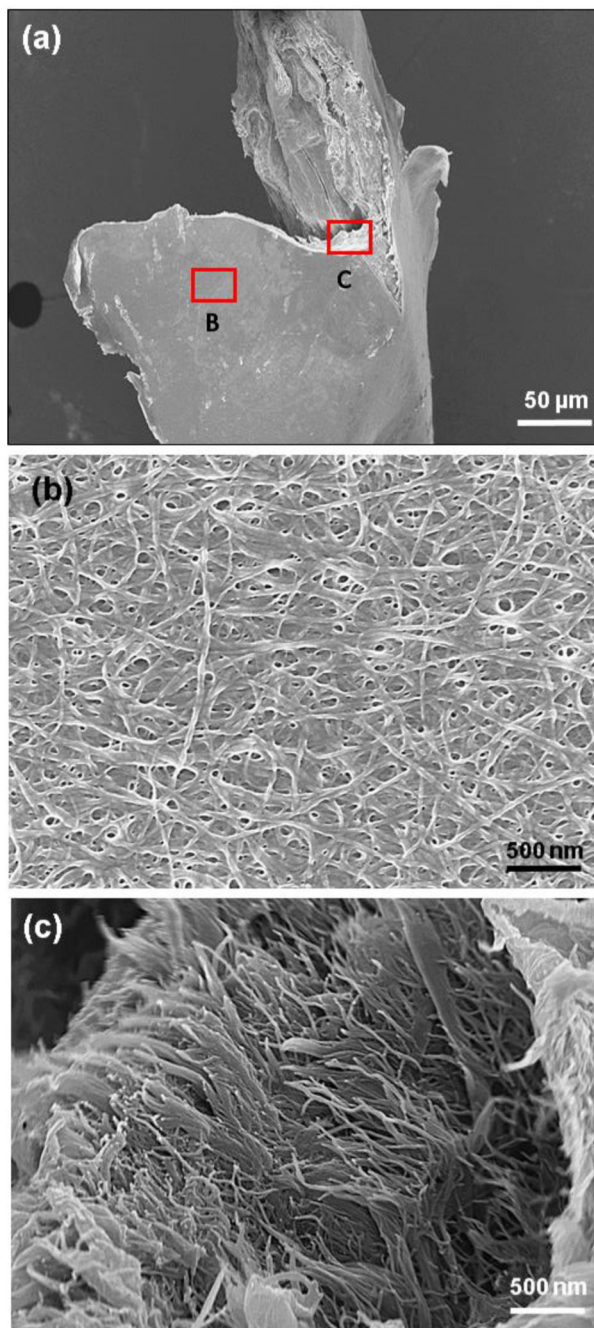


**Figure 7.** Electron microscopy images show the compaction of collagen fibers on surface and cross-section of compacted collagen sheet; a low magnification image of compacted collagen sheet showing the surface and cross-sectional topographies of sheets (a). Higher magnification image shows high degree of collagen fibril compaction on surface of sheets with nano scale porosity (b). Cross-sectional image illustrates the fibrous structure continue to the depth of sheet with same degree of compaction (c).

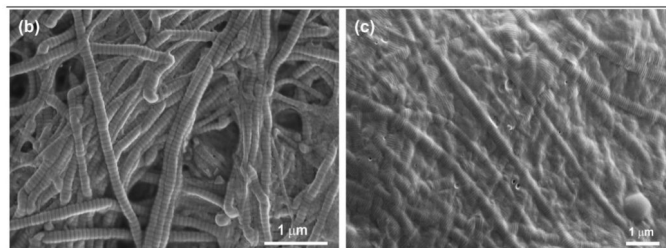
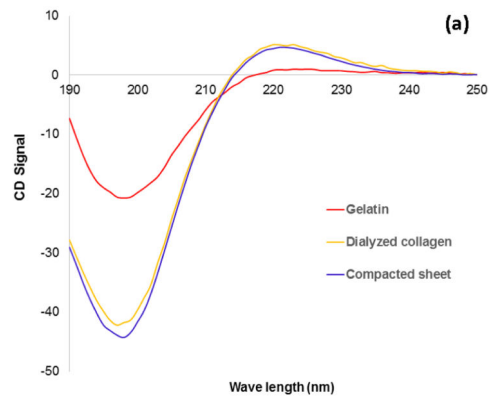


**Figure 8. Result of protein conformational analyses of electrocompacted collagen indicate that electrocompaction process does not harm the collagen**

(a) Results of circular dichroism illustrate the similarities between the spatial conformation of collagen before and after electrocompaction process while there is a big difference between the gelatin structures with collagen after electrocompaction. Electron microscope images confirm the results of two previous analyses visually. SEM images show the d-banding pattern of collagen (b) fibers are preserved after electrocompaction (c). Results of all two analyses confirm that the collagen microstructure is preserved after electrocompaction.